Cluster-shell competition and its effect on the $E0$ transition probability in ^{20}Ne

N. Itagaki[1] and H. Matsuno[2]
[1] *Yukawa Institute for Theoretical Physics, Kyoto University, Kitashirakawa Oiwake-Cho, Kyoto 606-8502, Japan*
[2] *Department of Physics, Kyoto University, Kitashirakawa Oiwake-Cho, Kyoto 606-8502, Japan*

(Dated: January 27, 2016)

^{20}Ne has been known as a typical example of a nucleus with α cluster structure (^{16}O+α structure). However according to the spherical shell model, the spin-orbit interaction acts attractively for four nucleons outside of the ^{16}O core, and this spin-orbit effect cannot be taken into account in the simple α cluster models. We investigate how the α cluster structure competes with independent particle motions of these four nucleons. The antisymmetrized quasi-cluster model (AQCM) is a method to describe a transition from the α cluster wave function to the jj-coupling shell model wave function. In this model, the cluster-shell transition is characterized by only two parameters; R representing the distance between clusters and Λ describing the breaking of α clusters, and the contribution of the spin-orbit interaction, very important in the jj-coupling shell model, can be taken into account by changing α clusters to quasi clusters. In this article, based on AQCM, we apply ^{16}O plus one quasi cluster model for ^{20}Ne. Here we focus on the $E0$ transition matrix element, which has been known as the quantity characterizing the cluster structure. The $E0$ transition matrix elements are sensitive to the change of the wave functions from α cluster to jj-coupling shell model.

PACS numbers: 21.60.Gx, 21.10.Ky

arXiv:1601.06900v1 [nucl-th] 26 Jan 2016

I. INTRODUCTION

^{20}Ne has been known as a typical example of a nucleus which has α cluster structure. There have been numerous works based on the cluster model, which explain the observed doublet rotational band structure. In addition to the ground $K^\pi = 0^+$ band, the negative parity band ($K^\pi = 0^-$) starting with the 1^- state at $E_x = 5.787726$ MeV has been observed, and existence of this "low-lying" negative parity band is the strong evidence that simple spherical mean field is broken. These bands are well explained by the picture that α cluster is located at some distance from the ^{16}O core [1]. Recently "container picture" has been proposed to describe the non-localization of the α cluster around ^{16}O [2].

However, according to the shell model, four nucleons perform independent particle motions around the ^{16}O core, which has doubly closed shell of the p shell, and the spin-orbit interaction acts attractively to them. If we apply simple α cluster models, we cannot take into account this spin-orbit effect. In traditional α cluster models, α cluster is defined as $(0s)^4$ configuration centered at some localized point, and the contributions of non-central interactions vanish. If we correctly take into account the spin-orbit effect, α cluster structure competes with the jj-coupling shell model structure. Previously we have investigated this competition in ^{20}Ne based on the antisymmetrized quasi-cluster model (AQCM) [3]. AQCM is a method that enables us to describe a transition from the α cluster wave function to the jj-coupling shell model wave function [4–8]. In this model, the cluster-shell transition is characterized by only two parameters; R representing the distance between α cluster and core nucleus and Λ describing the breaking of the α cluster. By introducing Λ, we transform α cluster to quasi cluster, and the contribution of the spin-orbit interaction, very important in the jj-coupling shell model, can be taken into account. It was found that the level structure of the yrast states of ^{20}Ne strongly depends on the strength of the spin-orbit interaction in the Hamiltonian.

In this article we apply AQCM again to ^{20}Ne and introduce ^{16}O plus one quasi cluster model. Particularly we focus on the effect of cluster-shell competition on the $E0$ transition. The $E0$ transition operator has the form of monopole operator, $\sum_i r_i^2$, and this operator changes the nuclear sizes. However, changing nuclear density uniformly requires quite high excitation energy. On the other hand, clusters structures are characterized as weakly interacting states of strongly bound subsystems. Thus it is rather easy for the cluster states to change the sizes without giving high excitation energies; this is achieved just by changing the relative distances between clusters. Therefore, $E0$ transitions in low-energy regions are expected to be signatures of the cluster structures, and many works along this line are going on [9–14].

In our preceding work for ^{16}O [15], we found that the ground state has a compact four α structure and is almost independent of the strength of the spin-orbit interaction; however the second 0^+ state, which has been known as a ^{12}C+α cluster state, is very much affected by the change of the strength. With increasing the strength, the level repulsion and crossing occur, and the ^{12}C cluster part changes from three α configuration to the $p_{3/2}$ subclosure of the jj-coupling shell model. The $E0$ transition matrix elements are strongly dependent on this level repulsion and crossing, and they are sensitive to the persistence of 4α correlation in the excited states. Here, "larger cluster" part of binary cluster system (^{12}C part of ^{12}C+α)

has been changed into quasi cluster. The present study on ^{20}Ne is different from the preceding work on ^{16}O in the following two points. One is that we focus on the change of "smaller cluster" part of the binary cluster system, and in this case, we change α cluster around the ^{16}O core to quasi cluster. Another difference is that this change influences very much the ground state (in the case of ^{16}O, the second 0^+ state with the ^{12}C+α configuration is affected by the spin-orbit interaction). Since other higher nodal states are determined by the orthogonal condition to the ground state, this change also has influences on the wave functions of the excited states. Naturally $E0$ transition matrix elements are also affected by this change.

The paper is organized as follows. The formulation is given in Sect. II. In Sect. III, the results for ^{20}Ne are shown. Finally, in Sect. IV we summarize the results and give the main conclusion.

II. FORMULATION

A. Wave function of the total system

The wave function of the total system Ψ is antisymmetrized product of these single particle wave functions;

$$\Psi = \mathcal{A}\{(\psi_1\chi_1\tau_1)(\psi_2\chi_2\tau_2)(\psi_3\chi_3\tau_3)\cdots\cdot(\psi_A\chi_A\tau_A)\}. \quad (1)$$

The projection onto parity and angular momentum eigen states can be numerically performed. The number of mesh points for the integral over Euler angles is 16^3.

B. Single particle orbits – ^{16}O part

For the single particle orbits of the ^{16}O part, we introduce conventional α cluster model. The single particle wave function has a Gaussian shape [16];

$$\phi_i = \left(\frac{2\nu}{\pi}\right)^{\frac{3}{4}} \exp\left[-\nu\left(\boldsymbol{r}_i - \boldsymbol{R}_i\right)^2\right]\eta_i, \quad (2)$$

where η_i represents the spin-isospin part of the wave function, and $\boldsymbol{R}_i$ is a real parameter representing the center of a Gaussian wave function for the ith particle. For the width parameter, we use the value of $b = 1.6$ fm, $\nu = 1/2b^2$. In this Brink-Bloch wave function, four nucleons in one α cluster share the common $\boldsymbol{R}_i$ value. Hence, the contribution of the spin-orbit interaction vanishes. We introduce four different kinds of $\boldsymbol{R}_i$ values, and four α clusters are forming tetrahedron configuration. When we take the limit of the relative distances between α cluster to zero, the wave function coincide with the closed p shell configuration of the shell model [16], and this limit is called Elliot SU(3) limit [17]. In our model, the relative distance is taken to be a small value, 0.1 fm.

C. Single particle orbits – one quasi cluster part

We add one quasi cluster around the ^{16}O core based on AQCM. In the AQCM, α clusters are changed into quasi clusters. For nucleons in the quasi cluster, the single particle wave function is described by a Gaussian wave packet, and the center of this packet $\boldsymbol{\zeta}_i$ is a complex parameter;

$$\psi_i = \left(\frac{2\nu}{\pi}\right)^{\frac{3}{4}} \exp\left[-\nu\left(\boldsymbol{r}_i - \boldsymbol{\zeta}_i\right)^2\right]\chi_i\tau_i, \quad (3)$$

$$\boldsymbol{\zeta}_i = \boldsymbol{R}_i + i\Lambda\boldsymbol{e}_i^{\rm spin} \times \boldsymbol{R}_i, \quad (4)$$

where χ_i and τ_i in Eq. (3) represent the intrinsic spin and isospin part of the ith single particle wave function, respectively. In Eq (4), $\boldsymbol{e}_i^{\rm spin}$ is a unit vector for the orientation of the intrinsic spin χ_i. Here, Λ is a real control parameter describing the dissolution of the α cluster. The width parameter is the same as nucleons in the ^{16}O cluster ($b = 1.6$ fm, $\nu = 1/2b^2$). As one can see immediately, the $\Lambda = 0$ AQCM wave function, which has no imaginary part, is the same as the conventional Brink-Bloch wave function. The AQCM wave function corresponds to the jj-coupling shell model wave function when $\Lambda = 1$ and $\boldsymbol{R}_i \to 0$. The mathematical explanation is summarized in Ref. [8].

Gaussian center parameters for the four nucleons in the quasi cluster ($\zeta_{17} \sim \zeta_{20}$) are given in the following way. Firstly. we place quasi cluster on the z axis, and the real part of the Gaussian center parameters ($\boldsymbol{R_{17\sim 20}}$) are given as

$$\boldsymbol{R_{17}} = \boldsymbol{R_{18}} = \boldsymbol{R_{19}} = \boldsymbol{R_{20}} = R\boldsymbol{e_z}. \quad (5)$$

Here R is a parameter, which describes the distance between quasi cluster and the ^{16}O cluster, and $\boldsymbol{e_z}$ is the unit vector in the z direction. Next, we give the imaginary parts. Here we quantize the spin of the nucleons along the x axis, and in order to satisfy the condition of Eq. (4), we must give the imaginary parts in the $-y$ direction as,

$$\boldsymbol{\zeta}_{17} = R(\boldsymbol{e_z} - i\Lambda\boldsymbol{e_y}), \quad (6)$$

$$\boldsymbol{\zeta}_{18} = R(\boldsymbol{e_z} + i\Lambda\boldsymbol{e_y}), \quad (7)$$

$$\boldsymbol{\zeta}_{19} = R(\boldsymbol{e_z} - i\Lambda\boldsymbol{e_y}), \quad (8)$$

$$\boldsymbol{\zeta}_{20} = R(\boldsymbol{e_z} + i\Lambda\boldsymbol{e_y}), \quad (9)$$

where e_z and e_y are unit vectors in the z and y direction, respectively. The Gaussian center parameter $\boldsymbol{\zeta}_{17}$ is for a proton with spin up ($+x$ direction), $\boldsymbol{\zeta}_{18}$ is for a proton with spin down ($-x$ direction), $\boldsymbol{\zeta}_{19}$ is for a neutron with spin up ($+x$ direction), and $\boldsymbol{\zeta}_{20}$ is for a neutron with spin down ($-x$ direction). When Λ is set to zero, the wave function consisting the quasi clusters agrees with that of an α cluster. If we take the limit of $R \to 0$ and $\Lambda = 1$, four nucleons in the quasi cluster occupy $d_{5/2}$ orbits of the jj-coupling shell model.

D. Hamiltonian

For the Hamiltonian, we use Volkov No.2 [18] as an effective interaction for the central part with the Majorana exchange parameter of $M = 0.62$. For the spin-orbit part, G3RS [19], which is a realistic interaction originally determined to reproduce the nucleon-nucleon scattering phase shift, is adopted;

$$\hat{V}_{spin-orbit} = V_{ls}(e^{-d_1 r^2} - e^{-d_2 r^2})P(^3O)\vec{L}\cdot\vec{S}, \quad (10)$$

where $d_1 = 5.0$ fm^{-2}, $d_2 = 2.778$ fm^{-2}, and $P(^3O)$ is a projection operator onto a triplet odd state. The operator $\vec{L}$ stands for the relative angular momentum and $\vec{S}$ is the spin ($\vec{S_1} + \vec{S_2}$). In the present work, the strength of the spin-orbit interaction, V_{ls}, is a parameter as in Ref. [15] and we compare the results by changing the value.

III. RESULTS

In this section, we apply our AQCM wave function introduced in the previous section to ^{20}Ne and discuss the V_{ls} (strength of the spin-orbit interaction) dependence of energy levels and $E0$ transition probabilities. The V_{ls} value is changed from 0 MeV to 3000 MeV, and reasonable value of around 1500 MeV has been suggested in our preceding work [3].

A. Energy of each GCM basis state

We prepare AQCM wave functions with different R and Λ values as basis states of generator coordinate method (GCM). The adopted values are $R = 1, 2, 3, 4, 5, 6, 7$ fm and $\Lambda = 0, 1/3, 2/3, 1$. The 0^+ energies of these basis states are presented in Table I, and here, we show the values for two extreme cases for the strengths of the spin-orbit interaction; (a) $V_{ls} = 0$ MeV and (b) $V_{ls} = 3000$ MeV. The 0^+ energies of the GCM basis states corresponding to other V_{ls} values can be estimated just by interpolating these values linearly.

In Table I (a), we find that $\Lambda = 0$ basis states give lower energies than Λ finite basis states. This is because of the absence of the spin-orbit interaction; introducing imaginary part for the Gaussian center parameters does not work for the spin-orbit interaction and that simply increases the kinetic energy of four nucleons in the quasi cluster. Here the basis state with $R = 3$ fm ($\Lambda = 0$) gives the lowest energy of -153.6 MeV.

On the contrary, Table I (b) is the case of $V_{ls} = 3000$ MeV, and basis states with finite Λ values get much lower, since the contribution of the spin-orbit interaction can be taken into account by transforming the α cluster to quasi cluster. The basis state which gives the lowest energy has the values of $\Lambda = 2/3$ and $R = 1$ fm (-163.8 MeV). This result suggests that when the spin-orbit interaction is switched on, the R value of the optimal basis state becomes smaller and the Λ value increases. This means that not only the α cluster dissolutes into quasi cluster, the relative distance between the cluster and the ^{16}O core decreases.

TABLE I: The 0^+ energies of GCM basis states for the cases of different strengths of the spin-orbit interaction; (a) $V_{ls} = 0$ MeV and (b) $V_{ls} = 3000$ MeV. The 0^+ energies of the GCM basis states with other V_{ls} values can be estimated by linearly interpolating these two.

(a)

R (fm)	$\Lambda = 0$	$\Lambda = 1/3$	$\Lambda = 2/3$	$\Lambda = 1$
1	-147.7	-141.8	-131.5	-128.1
2	-151.5	-144.1	-127.5	-111.7
3	-153.6	-141.2	-104.6	-50.0
4	-152.1	-129.4	-55.3	54.5
5	-148.2	-109.1	8.7	183.4
6	-144.5	-84.3	77.7	330.4
7	-142.7	-59.1	151.8	489.9

(b)

R (fm)	$\Lambda = 0$	$\Lambda = 1/3$	$\Lambda = 2/3$	$\Lambda = 1$
1	-147.7	-163.8	-164.2	-162.4
2	-151.5	-162.3	-155.9	-144.3
3	-153.6	-153.3	-124.6	-76.6
4	-152.1	-134.4	-63.6	41.3
5	-148.2	-108.3	9.9	182.6
6	-144.5	-80.2	83.0	334.5
7	-142.7	-53.6	158.8	503.5

B. 0^+ energies

We superpose these AQCM wave functions with different R and Λ values based on GCM. The 0^+ eigen energies and coefficients for the linear combination of the GCM basis states for each eigen state are obtained by diagonalizing the Hamiltonian (solving the Hill-Wheeler equation [16]). Here we change the strength of the spin-orbit interaction, V_{ls}, and diagonalize the Hamiltonian at each V_{ls} value.

The obtained 0^+ energy curves of ^{20}Ne as a function of V_{ls} are shown in Fig. 1. The ground state gets more binding with increasing V_{ls}; the 0^+ energy changes from -155.2 MeV ($V_{ls} = 0$ MeV) to -166.3 MeV ($V_{ls} = 3000$ MeV). These energies are lower than the ones for the optimal GCM basis states shown in Table I by about 2 MeV, and this is the effect of superposing the GCM basis states. The experimental value for the ground state is -160.6448 MeV.

In Fig. 1, we find that the fourth 0^+ state at $V_{ls} = 0$ starts lowering soon after the spin-orbit interaction is switched on, and the decrease of the energy is much steeper than other states. The level repulsion (crossing) between the fourth and the third 0^+ states occurs around $V_{ls} = 1000$ MeV, and here the wave functions of these two states strongly mix. There is another level repulsion (crossing) between this third and the second 0^+ state around $V_{ls} = 1500$ MeV. Because of these level

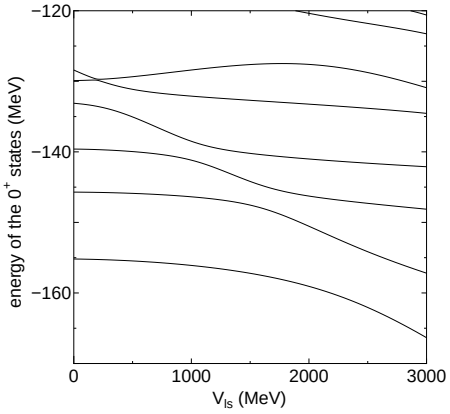

FIG. 1: The 0^+ energy curves of ^{20}Ne obtained by superposing the AQCM wave functions with $R = 1, 2, 3, 4, 5, 6, 7$ fm and $\Lambda = 0, 1/3, 2/3, 1$. The energy curves are plotted as a function of the strength of the spin-orbit interaction, V_{ls} in the Hamiltonian

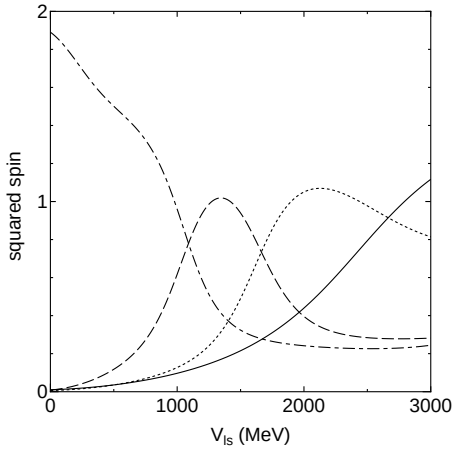

FIG. 2: The absolute value of the expectation values for the squared spin as a function of the strength of the spin-orbit interaction, V_{ls}. The solid, dotted, dashed, and dash-dotted lines are for the ground, second, third, and fourth 0^+ states of Fig. 1.

repulsions (crossings), it looks that the wave function of the fourth state at $V_{ls} = 0$ MeV comes down and mixes in the ground and second states at $V_{ls} = 3000$ MeV.

On the other hand, the wave function of the second 0^+ state at $V_{ls} = 0$ MeV almost stays at this energy even after the spin-orbit interaction is switched on. Around $V_{ls} = 1500$ MeV, the level repulsion (crossing) occurs and this wave function becomes the one for the third 0^+ state beyond this region, but the energy is almost constant even after that. Similar thing can be found for the third 0^+ state at $V_{ls} = 0$. After the level repulsion (crossing) around $V_{ls} = 1000$ MeV, this state corresponds to the fourth 0^+ state at $V_{ls} = 3000$ MeV. These two states are considered to return back to the α cluster structure beyond these level repulsion (crossing) regions.

C. Intrinsic spin

Next, we discuss the structure change of each 0^+ state as a function of V_{ls} by analyzing the spin structure. In the traditional cluster models, such as ^{16}O+α models, the clusters are spin saturated systems, and the expectation value of intrinsic spin operator ($\sum_i \vec{s}_i$, where $\vec{s}_i$ is the spin operator for the ith nucleon) becomes zero. However, in AQCM, α clusters are changed into quasi clusters, and the contribution of the spin-orbit interaction can be taken into account. In such case, the intrinsic spin structure of quasi cluster changes from that of α cluster as a function of Λ value. This can be proven by calculating the expectation values for the square of the intrinsic spin operator ($\sum_{i,j} \vec{s}_i \cdot \vec{s}_j$).

In Fig. 2, the absolute values of the expectation value for the squared spin are shown as a function of the strength of the spin-orbit interaction, V_{ls}. The solid, dotted, dashed, and dash-dotted lines are for the ground, second, third, and fourth 0^+ states of Fig. 1. At $V_{ls} = 0$ MeV, the ground, second, and third 0^+ states have squared spin zero; without the spin-orbit force, α cluster structure is not broken. On the contrary, the fourth 0^+ state has the value of 1.89. Here the α cluster structure is broken even without the spin-orbit interaction, and this is considered to be due to orthogonal condition to other lower states.

With increasing V_{ls}, the values for the first, second, and third 0^+ states start increasing. This corresponds to the fact that the spin-orbit interaction acts attractively for these states. Around $V_{ls} = 1000$ MeV, the dashed line and dash-dotted line cross, and this is due to the level repulsion (crossing) of the third and fourth states shown in Fig. 1. Also, this dashed line crosses with dotted line around $V_{ls} = 1500$ MeV, and this corresponds to the level repulsion (crossing) of the second and third states, as discussed in the previous subsection. Beyond this level repulsion region, the values for the third and fourth 0^+ states decrease, and α cluster components become important again in these states. The third and fourth 0^+ states go back to α cluster structure. On the contrary, the values for the first and second 0^+ states significantly increase around $V_{ls} = 2000$ MeV, and in this region, it is considered that the component of fourth 0^+ state at $V_{ls} = 0$ MeV strongly mix in these states.

D. Squared overlap between the final solution and each GCM basis state

Next we discuss the character of each state by showing the squared overlap between the final solution and each GCM basis state. In Table II, the absolute values of the squared overlaps between the final solution and each GCM basis state in the case of $V_{ls} = 0$ MeV are shown. These are the results when the spin-orbit interaction is

TABLE II: The absolute values of the squared overlaps between the final solution and each GCM basis state in the case of $V_{ls} = 0$ MeV. (a) is for the ground 0^+ state (-155.2 MeV), (b) is for the second 0^+ state (-145.7 MeV), (c) is for the third 0^+ state (-139.6 MeV), and (d) is for the fourth 0^+ state (-133.1 MeV).

(a)

R (fm)	$\Lambda = 0$	$\Lambda = 1/3$	$\Lambda = 2/3$	$\Lambda = 1$
1	0.57	0.35	0.07	0.03
2	0.74	0.45	0.08	0.02
3	0.92	0.53	0.07	0.01
4	0.83	0.39	0.02	0.00
5	0.43	0.13	0.00	0.00
6	0.11	0.02	0.00	0.00
7	0.02	0.00	0.00	0.00

(b)

R (fm)	$\Lambda = 0$	$\Lambda = 1/3$	$\Lambda = 2/3$	$\Lambda = 1$
1	0.17	0.12	0.03	0.01
2	0.15	0.09	0.02	0.00
3	0.04	0.03	0.01	0.00
4	0.03	0.01	0.00	0.00
5	0.41	0.11	0.00	0.00
6	0.74	0.11	0.00	0.00
7	0.53	0.03	0.00	0.00

(c)

R (fm)	$\Lambda = 0$	$\Lambda = 1/3$	$\Lambda = 2/3$	$\Lambda = 1$
1	0.14	0.10	0.03	0.21
2	0.08	0.06	0.02	0.01
3	0.00	0.01	0.00	0.00
4	0.08	0.03	0.00	0.00
5	0.12	0.03	0.00	0.00
6	0.02	0.00	0.00	0.00
7	0.43	0.02	0.00	0.00

(d)

R (fm)	$\Lambda = 0$	$\Lambda = 1/3$	$\Lambda = 2/3$	$\Lambda = 1$
1	0.00	0.32	0.33	0.23
2	0.00	0.34	0.32	0.16
3	0.00	0.27	0.17	0.03
4	0.00	0.12	0.03	0.00
5	0.00	0.02	0.00	0.00
6	0.00	0.00	0.00	0.00
7	0.00	0.00	0.00	0.00

TABLE III: The absolute values of the squared overlaps between the final solution and each GCM basis state in the case of $V_{ls} = 3000$ MeV. (a) is for the ground 0^+ state (-166.3 MeV), (b) is for the second 0^+ state (-157.2 MeV), (c) is for the third 0^+ state (-148.1 MeV), and (d) is for the fourth 0^+ state (-142.1 MeV).

(a)

R (fm)	$\Lambda = 0$	$\Lambda = 1/3$	$\Lambda = 2/3$	$\Lambda = 1$
1	0.33	0.84	0.88	0.74
2	0.32	0.79	0.74	0.49
3	0.27	0.53	0.32	0.07
4	0.13	0.18	0.00	0.00
5	0.03	0.02	0.00	0.00
6	0.00	0.00	0.00	0.00
7	0.00	0.00	0.00	0.00

(b)

R (fm)	$\Lambda = 0$	$\Lambda = 1/3$	$\Lambda = 2/3$	$\Lambda = 1$
1	0.32	0.08	0.10	0.21
2	0.42	0.14	0.05	0.11
3	0.49	0.21	0.00	0.00
4	0.40	0.17	0.00	0.00
5	0.18	0.06	0.00	0.00
6	0.04	0.01	0.00	0.00
7	0.00	0.00	0.00	0.00

(c)

R (fm)	$\Lambda = 0$	$\Lambda = 1/3$	$\Lambda = 2/3$	$\Lambda = 1$
1	0.04	0.05	0.00	0.01
2	0.01	0.02	0.00	0.01
3	0.03	0.01	0.01	0.00
4	0.32	0.13	0.01	0.00
5	0.67	0.20	0.00	0.00
6	0.57	0.09	0.00	0.00
7	0.24	0.01	0.00	0.00

(d)

R (fm)	$\Lambda = 0$	$\Lambda = 1/3$	$\Lambda = 2/3$	$\Lambda = 1$
1	0.00	0.01	0.00	0.00
2	0.01	0.00	0.00	0.00
3	0.06	0.02	0.01	0.00
4	0.10	0.05	0.00	0.00
5	0.00	0.00	0.00	0.00
6	0.26	0.03	0.00	0.00
7	0.67	0.04	0.00	0.00

switched off, and (a) is for the ground 0^+ state (-155.2 MeV), (b) is for the second 0^+ state (-145.7 MeV), (c) is for the third 0^+ state (-139.6 MeV), and (d) is for the fourth 0^+ state (-133.1 MeV). As shown in Table II (a), the ground 0^+ state has the squared overlap of 0.92 with the GCM basis state which has $R = 3$ fm and $\Lambda = 0$. The second 0^+ state is a higher nodal state and has much larger ^{16}O-α distance than the ground state; this is due to the orthogonal condition to the ground state. As shown in Table II (b), the state has the squared overlap of 0.74 (0.53) with the GCM basis state which has $R = 6$ (7) fm and $\Lambda = 0$. The third 0^+ state also has large ^{16}O-α distance (Talbe II (c)). The fourth 0^+ state has overlaps with basis states with finite Λ values (Table II (b)). However, since the spin-orbit interaction is absent ($V_{ls} = 0$ MeV), the excitation energy is rather large ($E_x \sim 22.1$ MeV).

We move on to another extreme case that the strength of the spin-orbit interaction is set to $V_{ls} = 3000$ MeV. In Table III, the absolute values of the squared overlaps between the final solution and each GCM basis state in the case of $V_{ls} = 3000$ MeV are shown. Here (a) is for the ground 0^+ state (-166.3 MeV), (b) is for the second 0^+ state (-157.2 MeV), (c) is for the third 0^+ state (-148.1 MeV), and (d) is for the fourth 0^+ state (-142.1 MeV). As shown in Table III (a), the ground 0^+ state has the squared overlap of 0.88 with the GCM basis state which has $R = 1$ fm and $\Lambda = 2/3$. The R value becomes very small and Λ value increased compared with the case of $V_{ls} = 0$ MeV, as expected in the previous subsection. The α cluster structure is completely washed out. The second 0^+ state is no longer a higher nodal state of ^{16}O+α with

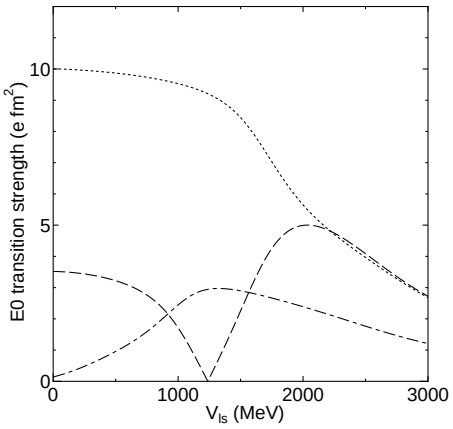

FIG. 3: The $E0$ transition matrix elements from the ground state. The dotted, dashed, and dash-dotted lines show the ones to the second, third, and fourth 0^+ states.

large relative distance, because of the level crossing when increasing the V_{ls} value. As shown in Table III (b), although the state still has the squared overlap of 0.49 with the GCM basis state which has $R = 3$ fm and $\Lambda = 0$, the squared overlaps with finite Λ basis states increase. The third and fourth 0^+ states have overlaps with basis states with large R values; the third state has 0.67 with $R = 5$ fm $\Lambda = 0$ (Table III (c)), and the forth state has 0.67 with $R = 7$ fm $\Lambda = 0$ (Table III (d)). The character of the second and third 0^+ states at $V_{ls} = 0$ MeV remains here, as expected in the previous subsection.

E. $E0$ transition matrix elements

The $E0$ transition matrix elements from the ground state are shown in Fig. 3. The dotted, dashed, and dash-dotted lines show the ones to the second, third, and fourth 0^+ states. The operator has the form of $e\sum_i r_i^2$, and summation is for protons. The experimental value form the ground state to the second 0^+ state is 6.914 e fm^2. The calculated value (dotted line) at $V_{ls} = 0$ MeV is 10.0 e fm^2, and this is slightly larger. As we discussed in Table II (a) and (b), when the spin-orbit interaction is switched off, both ground and second 0^+ states have α cluster structure, and the second 0^+ state has spatially more extended distribution. In this case the matrix element of the $E0$ transition between these states becomes large. With increasing the V_{ls} value, the mixing of basis states with finite Λ values becomes important in both the ground and second 0^+ states, and the $E0$ transition matrix decreases. The value agrees with the experimental one around $V_{ls} = 1770$ MeV. In our preceding work [3], we deduced proper strength for the spin-orbit interaction from the analyses on the level structure, and the present result is almost similar to this one.

As shown in Fig. 3, around $V_{ls} = 1000 \sim 1500$ MeV region, the dashed line and dash-dotted line cross, reflecting the fact that the level repulsion (crossing) of the third and fourth states occurs. The wave functions are interchanged in this region. Also, this dashed line crosses with the dotted line around $V_{ls} = 2000$ MeV, and this corresponds to the level repulsion (crossing) between the third and second and states as discussed in the previous subsection.

Now we analyze the wave function of each 0^+ state calculated using the spin-orbit strength which reproduces the experimental $E0$ transition probability from the ground state to the second 0^+ state. The absolute value of the squared overlap between the final solution and each GCM basis state in the case of $V_{ls} = 1770$ MeV is shown in Table IV; (a) is for the ground 0^+ state

TABLE IV: The absolute values of the squared overlaps between the final solution and each GCM basis state in the case of $V_{ls} = 1770$ MeV, which gives a reasonable $E0$ transition matrix element from the ground state to the second 0^+ state. (a) is for the ground 0^+ state (-158.1 MeV), (b) is for the second 0^+ state (-148.9 MeV), (c) is for the third 0^+ state (-145.5 MeV), and (d) is for the fourth 0^+ state (-140.7 MeV).

(a)

R (fm)	$\Lambda = 0$	$\Lambda = 1/3$	$\Lambda = 2/3$	$\Lambda = 1$
1	0.62	0.74	0.33	0.20
2	0.73	0.82	0.33	0.15
3	0.78	0.75	0.19	0.03
4	0.57	0.40	0.03	0.00
5	0.23	0.09	0.00	0.00
6	0.05	0.01	0.00	0.00
7	0.01	0.00	0.00	0.00

(b)

R (fm)	$\Lambda = 0$	$\Lambda = 1/3$	$\Lambda = 2/3$	$\Lambda = 1$
1	0.00	0.18	0.49	0.50
2	0.00	0.11	0.38	0.32
3	0.07	0.01	0.12	0.04
4	0.26	0.04	0.00	0.00
5	0.40	0.09	0.00	0.00
6	0.27	0.04	0.00	0.00
7	0.10	0.01	0.00	0.00

(c)

R (fm)	$\Lambda = 0$	$\Lambda = 1/3$	$\Lambda = 2/3$	$\Lambda = 1$
1	0.11	0.00	0.15	0.23
2	0.10	0.00	0.12	0.14
3	0.04	0.00	0.05	0.02
4	0.01	0.02	0.01	0.00
5	0.24	0.08	0.00	0.00
6	0.47	0.07	0.00	0.00
7	0.36	0.02	0.00	0.00

(d)

R (fm)	$\Lambda = 0$	$\Lambda = 1/3$	$\Lambda = 2/3$	$\Lambda = 1$
1	0.05	0.04	0.00	0.02
2	0.01	0.01	0.01	0.01
3	0.01	0.00	0.01	0.00
4	0.11	0.05	0.00	0.00
5	0.06	0.02	0.00	0.00
6	0.08	0.01	0.00	0.00
7	0.49	0.03	0.00	0.00

(−158.1 MeV), (b) is for the second 0^+ state (−148.9 MeV), (c) is for the third 0^+ state (−145.5 MeV), and (d) is for the fourth 0^+ state (−140.7 MeV). The ground state has the squared overlap with the α cluster state; the value for the basis state with $R = 3$ fm and $\Lambda = 0$ is 0.78, and the character at $V_{ls} = 0$ MeV still remains. However the largest squared overlap of 0.82 is with the basis state which has $R = 2$ fm and $\Lambda = 1/3$. Therefore, the α breaking effect due to the spin-orbit interaction is important. The second 0^+ states was very extended ^{16}O+α cluster state at $V_{ls} = 0$ MeV, and the second state at $V_{ls} = 1770$ MeV still has the squared overlap of 0.40 with the basis state which has $R = 5$ fm and $\Lambda = 0$. However, at $V_{ls} = 1770$ MeV the state also has components of the basis states with finite Λ values; the squared overlap with the basis state $R = 1$ fm and $\Lambda = 1$ is 0.50. The third and fourth 0^+ states at $V_{ls} = 1770$ MeV contain the components of α cluster structure ($\Lambda = 0$) with large R values.

F. 1^- states

We move on from 0^+ states to 1^- states, and the energy curves of 1^- states ($K = 0$) as a function of V_{ls} are shown in Fig. 4. The presence of low-lying negative parity band starting with the first 1^- has been the key evidence for the α cluster structure. The present result shows that the energy of this first 1^- state is almost constant even if the spin-orbit interaction is switched on. This means that α breaking basis states do not contribute and the α cluster structure is really important in this state. The absolute values of the squared overlaps between the first 1^- state and each GCM basis state are shown in Table V. Table V (a) is the case of $V_{ls} = 0$ MeV, which gives −150.3 MeV for the first 1^- state. The largest squared overlap of 0.89 is with the base state which has $R = 4$ fm and $\Lambda = 0$. This character remains in Table V (b), which is the case of $V_{ls} = 3000$ MeV. The first 1^- state is obtained at −152.0 MeV, and the largest squared overlap of 0.85 is with the base state which has $R = 4$ fm and $\Lambda = 0$. Even in the case of quite strong spin-orbit interaction, the α cluster structure remains in the first 1^- state.

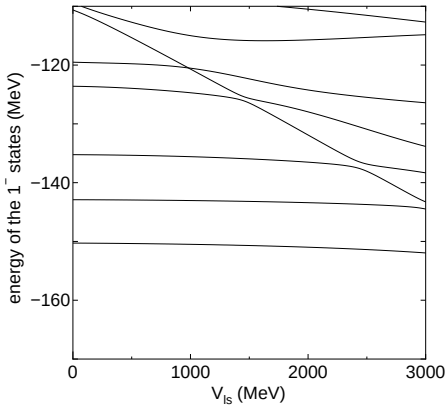

FIG. 4: The 1^- energy curves of ^{20}Ne obtained by superposing the AQCM wave functions with $R = 1, 2, 3, 4, 5, 6, 7$ fm and $\Lambda = 0, 1/3, 2/3, 1$. The energy curves are plotted as a function of the strength of the spin-orbit interaction, V_{ls} in the Hamiltonian

TABLE V: The absolute values of the squared overlaps between the first 1^- state and each GCM basis state. (a) is at $V_{ls} = 0$ MeV and 1^-_1 is obtained at −150.3 MeV. (b) is at $V_{ls} = 3000$ MeV and 1^-_1 is obtained at −152.0 MeV..

(a)

R (fm)	$\Lambda = 0$	$\Lambda = 1/3$	$\Lambda = 2/3$	$\Lambda = 1$
1	0.28	0.14	0.02	0.00
2	0.41	0.21	0.03	0.00
3	0.64	0.32	0.03	0.00
4	0.89	0.39	0.02	0.00
5	0.81	0.24	0.00	0.00
6	0.40	0.06	0.00	0.00
7	0.11	0.01	0.00	0.00

(b)

R (fm)	$\Lambda = 0$	$\Lambda = 1/3$	$\Lambda = 2/3$	$\Lambda = 1$
1	0.40	0.40	0.11	0.03
2	0.53	0.50	0.13	0.03
3	0.73	0.60	0.10	0.01
4	0.85	0.53	0.03	0.00
5	0.62	0.23	0.00	0.00
6	0.24	0.04	0.00	0.00
7	0.05	0.00	0.00	0.00

IV. SUMMARY

We have applied AQCM, which is a method to describe a transition from the α-cluster wave function to the jj-coupling shell model wave function, to ^{20}Ne. ^{20}Ne has been known as a nucleus which has ^{16}O+α structure, and we investigated how the α cluster structure competes with independent particle motions of these four nucleons by changing the strength of the spin-orbit interaction (V_{ls}). We focused on the $E0$ transition matrix element, which was found to be sensitive to V_{ls}.

Based on AQCM, ^{20}Ne is characterized by only two parameters; R representing the relative distance between ^{16}O and α and Λ describing the breaking of α cluster. When the spin-orbit interaction is switched off ($V_{ls} = 0$ MeV), the ground 0^+ state has the squared overlap of 0.92 with the GCM basis state which has $R = 3$ fm and $\Lambda = 0$. The second 0^+ state is a higher nodal state and it has 0.74 with $R = 6$ fm and $\Lambda = 0$. The third 0^+ state also has large ^{16}O-α distance, and the fourth 0^+ state has overlaps with basis states with finite Λ values.

When the spin-orbit interaction is switched on, we found that the decrease of the energy for the fourth 0^+ state at $V_{ls} = 0$ is much steeper than other states. Eventually the wave function of the fourth 0^+ state at $V_{ls} = 0$ MeV strongly mixes in the ground and second 0^+ states at $V_{ls} = 3000$ MeV. On the other hand, the wave function of the second 0^+ state at $V_{ls} = 0$ MeV almost stays

at this energy. Similar thing can be found for the third 0^+ state at $V_{ls} = 0$ MeV. These two states correspond to the third and fourth 0^+ states at $V_{ls} = 3000$ MeV, and α cluster structure becomes important again there.

The $E0$ transition matrix elements from the ground state to the second 0^+ state is calculated as 10.0 e fm^2 at $V_{ls} = 0$ MeV, which is slightly larger than the experimental value (6.914 e fm^2). With increasing V_{ls} value, the mixing of basis states with finite Λ values becomes important in both the ground and second 0^+ states, and the $E0$ transition matrix decreases. The value agrees with the experimental one around $V_{ls} = 1770$ MeV. This deduced strength is consistent with our preceding work on the level structure of this nucleus.

At $V_{ls} = 1770$ MeV, which is the spin-orbit strength deduced from the present analysis on the $E0$ transition matrix element, the ground state has the squared overlap of 0.78 with the basis state which has $R = 3$ fm and $\Lambda = 0$, and the character at $V_{ls} = 0$ MeV still remains. However the largest squared overlap of 0.82 is with the basis state which has $R = 2$ fm and $\Lambda = 1/3$. Therefore, the α breaking effect due to the spin-orbit interaction is also important in the ground state. The second 0^+ states has squared overlap of 0.40 with the basis state which has $R = 5$ fm and $\Lambda = 0$; however, it has also components of the basis states with finite Λ values. The third and fourth 0^+ states are α cluster states and contain the components of basis states with large R values.

The presence of low-lying negative parity band starting with the first 1^- has been the key evidence for the α cluster structure. We also investigated the 1^- states and found that the energy of the first 1^- state is almost constant even if the spin-orbit interaction is switched on and α breaking basis states are introduced. The α cluster structure is really important in this state.

There have been discussions that the ^{12}C+α+α cluster states appear in this energy region of the third 0^+ state, and inclusion of this configuration can be done by applying AQCM to the three α clusters in the ^{16}O core. Also, here we transformed an α cluster to four independent nucleons, in which the spin-orbit interaction acts attractively. However, in principle it is possible to introduce other shell model configurations, for instance configurations where the spin-orbit interaction acts repulsively, or one of the nucleon is excited from j-upper orbit to j-lower orbit. The analysis aiming at the unified view is going on.

Acknowledgments

Numerical calculation has been performed at Yukawa Institute for Theoretical Physics, Kyoto University.

[1] Hisashi Horiuchi and Kiyomi Ikeda, Prog. Theor. Phys. (1968) **40** 277.
[2] Bo Zhou, Zhongzhou Ren, Chang Xu, Y. Funaki, T. Yamada, A. Tohsaki, H. Horiuchi, P. Schuck, and G. Röpke, Phys. Rev. C **86**, 014301 (2012).
[3] N. Itagaki, J. Cseh, and M. Płoszajczak, Phys. Rev. C **83**, 014302 (2011).
[4] N. Itagaki, H. Masui, M. Ito, and S. Aoyama, Phys. Rev. C **71** 064307 (2005).
[5] H. Masui and N. Itagaki, Phys. Rev. C **75** 054309 (2007).
[6] T. Yoshida, N. Itagaki, and T. Otsuka, Phys. Rev. C **79** 034308 (2009).
[7] T. Suhara, N. Itagaki, J. Cseh, and M. Płoszajczak, Phys. Rev. C **87**, 054334 (2013).
[8] N. Itagaki, H. Matsuno, and T. Suhara, arXiv: 1507.02400.
[9] T. Kawabata *et al.*, Phys. Lett. B **646**, 6 (2007).
[10] Y. Sasamoto *et al.*, Mod. Phys. Lett. A **21**, 2393 (2006).
[11] T. Yoshida, N. Itagaki, and T. Otsuka, Phys. Rev. C **79**, 034308 (2009).
[12] Taiichi Yamada and Yasuro Funaki, Phys. Rev. C **92**, 034326 (2015).
[13] T. Ichikawa, N. Itagaki, T. Kawabata, Tz. Kokalova and W. von Oertzen, Phys. Rev. C **83**, 061301(R) (2011).
[14] T. Ichikawa, N. Itagaki, Y. Kanada-En'yo, Tz. Kokalova, and W. von Oertzen, Phys. Rev. C **86**, 031303(R) (2012).
[15] H. Matsuno and N. Itagaki, arXiv: 1601.05892.
[16] D. M. Brink, in *Proceedings of the International School of Physics "Enrico Fermi" Course XXXVI*, edited by C. Bloch (Academic, New York, 1966), p. 247.
[17] J. P. Elliot, Proc. Roy. Soc. A **245** 128, 562 (1958)
[18] A. B. Volkov, Nucl. Phys. **74**, 33 (1965).
[19] R. Tamagaki, Prog. Theor. Phys. **39**, 91 (1968).